Structural analysis of a stone arch bridge under incremental railway static loading

Rúben Silva

CONSTRUCT-LESE, Faculty of Engineering (FEUP), University of Porto

Cristina Costa

CONSTRUCT-LESE, Faculty of Engineering (FEUP), University of Porto

Polytechnic Institute of Tomar

António Arêde, Rui Calçada

CONSTRUCT-LESE, Faculty of Engineering (FEUP), University of Porto

Daniel Oliveira

ISISE, School of Engineering, University of Minho

Contacting author: rubenfsilva@fe.up.pt

Abstract

This paper reports on the modelling strategies used to represent the structural behaviour of a masonry single-arch railway bridge. The bridge structural behaviour is simulated by a 3D finite element model, in which the different bridge components are represented by homogeneous materials. The material nonlinear behaviour is simulated using a Drucker-Prager model. The assigned material properties are based on material testing, performed in similar stone masonry structures. The load-carrying capacity is evaluated using a 3D Ansys model and with a RING model of the bridge under incremental static loading representing normal railway traffic with appropriate configurations on the bridge deck, and the results compared.

Keywords: Railway bridges, FE numerical modelling, Constitutive material parameters, Load-carrying capacity

1. Introduction

Masonry arch bridges represent a significant percentage across the European railway networks. In Europe, masonry arch bridges are the most common railway bridge typology, and about 65 % of these bridges are older than 100 years and almost 75 % have spans less than 10 meters. Specifically, in Portugal, the number of masonry bridges represents 33% of the bridge stock, and the vast majority of masonry bridges, 79%, are short-span bridges [1].

The representativeness of this type of bridges in the network infrastructure and the growing need for expansion, higher capacity and new requirements of people and freight mobility are issues of major importance justifying a better understanding of the structural behaviour and assessment methodologies of masonry bridges. Numerical modelling strategies allow evaluating

the structural response of masonry bridges with realistic service and limit loading conditions, settlements, material and structural composition, thus contributing to help in the assessment of the bridge condition and in the implementation of suitable management plans for this type of bridges.

Finite element modelling strategies representing the nonlinear mechanical behaviour of the masonry components can be based on different levels of material representation, namely the so-called micro-models and the continuous homogeneous models. Regarding the continuous models, an equivalent continuum is defined with material characteristics that allow the representation of the masonry global behaviour as a composite material. In general, the material behaviour is considered isotropic. The constitutive laws are established in terms of stresses and strains, and different options to formulate the problem can be followed such as plastic models or damage models. Continuous homogeneous models can also be used to represent the infill material. For the assessment of the load-carrying capacity, these strategies require a good definition of the material models that should simulate adequately the materials' nonlinear behaviour.

In this paper, a nonlinear modelling strategy resorting to FE continuous homogeneous models is applied to Leça railway bridge, for its load-carrying assessment under incremental static loading. Since no experimental testing was performed for mechanical characterization of the bridge materials, a hypothetical scenario for material constitution was defined based on modelling parameters of a similar stone masonry railway bridge, the PK124 bridge, where a detailed experimental campaign was performed for material characterization. The details of this campaign and the obtained results can be found in another paper published by the same authors [2].

2. Bridge model

2.1 Brief description

The bridge over river Leça, illustrated in Figure 1, was built in granite stone and inaugurated in 1875 in Minho line. It is a single arch bridge with a span of 16 meters, with 18 meters high and 5.31 meters

width. The arch granite stone voussoirs have a thickness of about 1 meter. At the structure upstream and downstream, the bridge is restrained by granite stone masonry wing-walls, sustaining embankments. During the 1990's a new bridge (upstream of Leça bridge) was built in reinforced concrete with the purpose of duplicating the track in this section of Minho line. The stone masonry bridge deck supports one single track, consisting of concrete monoblock sleepers and UIC60 type rails resting on a variable height ballast layer.

Figure 1. Leça railway bridge

The geometric characterization of the bridge was based on visual inspections and by consulting the original drawings of the bridge design elements, as the example in Figure 2.
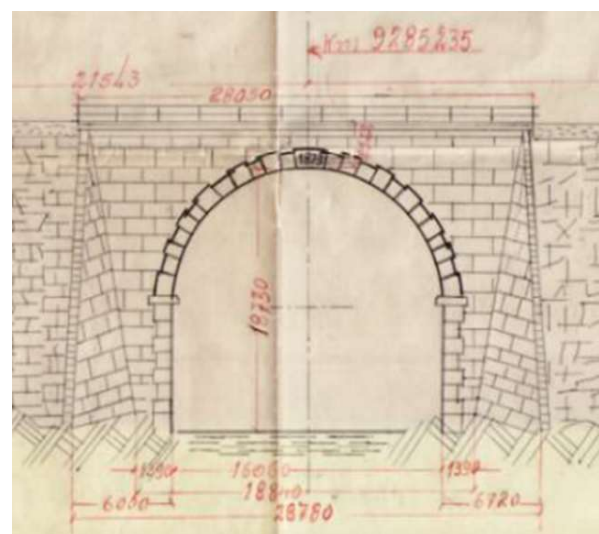

Figure 2. Design drawing of Leça bridge

2.2 FE bridge model

The definition of the bridge numerical model involved three different programs, Autocad [3], GID [4] and Ansys [5]. The bridge geometric model was defined in Autocad considering each bridge element according to the original design data. All elements were imported and meshed in GID software. The final model exported to ANSYS is illustrated in Figure 3. The model consists of solid type elements, SOLID 185, for the bridge structural components, and beam type elements, BEAM 188, for the rails.
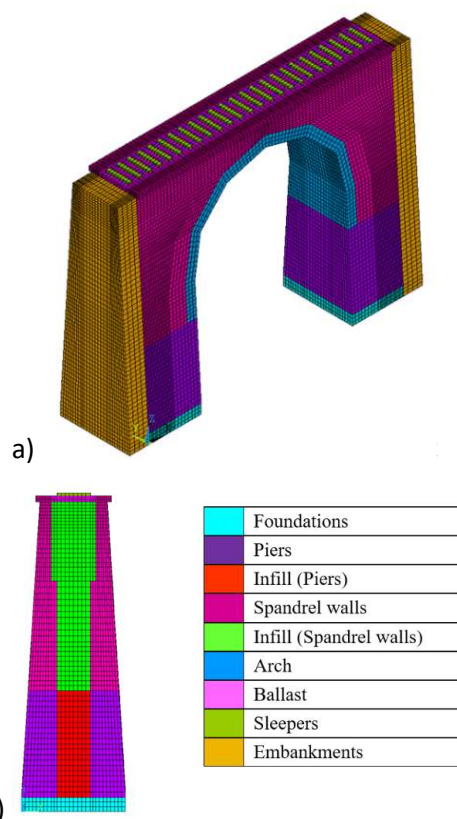

a)

	Foundations
	Piers
	Infill (Piers)
	Spandrel walls
	Infill (Spandrel walls)
	Arch
	Ballast
	Sleepers
	Embankments

b)

Figure 3. 3D ANSYS numerical model of Leça bridge: a) perspective, b) transverse section

The boundary conditions were set using rigid supports to fix the displacement X (longitudinal), Y (transversal) and Z (vertical) of the mesh nodes located at the base of the foundations, and rigid supports in the Y-direction in the nodes, which represent the contact with the wing walls. Additionally, two embankments were added in both lateral extremities of the model to simulate the confinement of the bridge in the longitudinal direction, which displacements in the external nodes of the Y-Z plane were also fixed in the X-

direction. The complete model consists of 128680 FE elements.

The masonry elements were modelled using a homogeneous composite material with equivalent mechanical properties so as to reproduce the properties of the assembly formed by stone blocks and mortar. The materials' nonlinear behaviour was simulated using the Drucker-Prager model available in ANSYS software.

2.3 Load modelling

The bridge structural response was evaluated under the influence of its self-weight and incremental static loading with vertical loads along the bridge deck.

The static loading scheme used in the bridge analysis is represented by the load model LM71 proposed by UIC to simulate the envelope of several types of trains. The load configuration of the LM71 model is also used as a design load for railway bridges according to Eurocodes [6] with the characteristic values shown in Figure 4 for bridges in rail tracks with normal traffic.
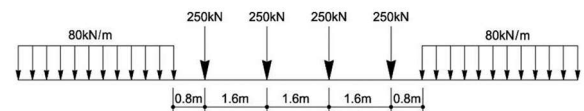

Figure 4. Load model LM71

The vehicle load position was defined from the most unfavourable position in the arch. For maximizing the deformations in the principal arch, the uniform load of the LM71 model was not considered. The vehicle load position was placed in the rail beam elements near the ¼ span of the arch. The loading history includes an initial phase of equilibrium of the dead load which was applied incrementally. After the first phase, the vehicle loading was applied considering incremental levels of intensity.

3. Material parameters

3.1 Experimental characterization of materials

The PK124 railway bridge is a culvert-type bridge constructed in 1879, located in Minho line of the

Portuguese railways. It is a short masonry bridge, consisting of one single arch with 11 m length. The PK124 bridge has age and weathered material conditions similar to those of the Leça bridge.

The in-situ experimental campaign carried out in PK124 bridge comprised core extraction of masonry joints and stone samples for lab testing, Ménard pressuremeter tests (PMT) in the infill material and single and double flat-jack tests in the masonry components. These tests were performed in the bridge abutment zone as shown in Figure 5. The laboratory tests involved the mechanical characterization of the granite stone and the masonry joints [2].
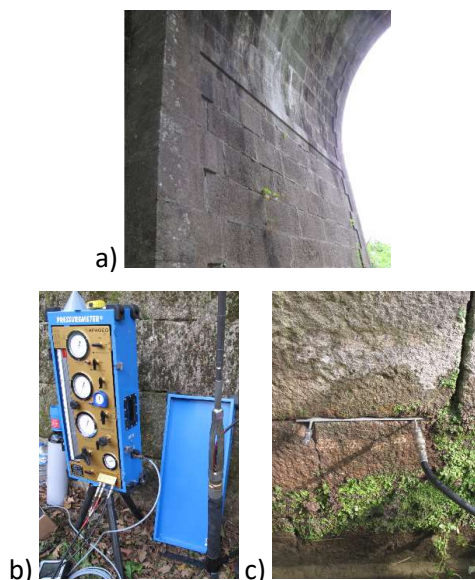

Figure 5. PK124 railway bridge: a) abutment and arch intrados b) Ménard pressuremeter and c) Flat-jack test

Aiming for calibration and validation the Drucker-Prager material parameters adopted in the masonry and infill bridge modelling, the simulation of the double flat-jack and pressuremeter tests was carried out using nonlinear modelling strategies similar to those used in the bridges. The material parameters assigned to the flat-jack and pressuremeter test models were adjusted to obtain good agreement between the experimental parameters and the corresponding parameters obtained by numerical simulation [7]. Finally, the calibrated Drucker-Prager parameters were also used to define the bridge material parameters.

3.2   Material properties

As a result of the strategy described in the previous paragraphs, the elastic material properties of the masonry (in the bridge zones of foundations, piers, arch and spandrel walls) and infill (in the backfill zones) are characterized by the elastic modulus, Poisson's ratio and unit weight listed in Table 1. The elastic characteristics of the ballast, sleepers, embankments and rails are also summarized in Table 1.

Table 1. Elastic parameters of the bridge materials

Parameter	Material	Adopted value	Unit
Elastic modulus	Masonry	2.0	GPa
	Infill	0.32	
	Embankments	0.2	
	Ballast	0.15	
	sleepers	36.0	
	Rail	210.0	
Unit weight	Masonry	24.5	kN/m³
	Infill	21.5	
	Embankments	21.5	
	Ballast	20.0	
	sleepers	28.9	
	Rail	78.5	
Poisson's ratio	all	0.2	-

For the nonlinear behaviour of the masonry and infill materials, the Drucker-Prager model was defined considering an elastic-plastic behaviour with the friction angle, cohesion, and dilatation angle summarized in Table 2. Which definition was based on the experimental characterization and numerical simulations of the flat-jack and the pressuremeter tests referred previously.

Table 2. Drucker-Prager parameters of masonry and infill

Parameter	Material	Adopted value	Unit
Cohesion	Masonry	450	kPa
	Infill	450	kPa
Friction angle	Masonry	35.5	°
	Infill	35.5	°
Dilatation angle	Masonry and infill	17.75	°

4. Analysis of the bridge response

This section focuses on the bridge response considering the nonlinear behaviour of the bridge materials and intensity load levels (multipliers) of the LM71 load pattern. The evolution of the structural response of the 3D FE model concerning the effect of the dead load and the vehicle load is presented and discussed for different levels of incremental intensity of the vertical load pattern.

A first estimation of the load carrying-capacity was obtained resorting to RING code [8] and considering several loading positions with the LM71 load pattern traveling through the entire bridge model. The program returns an adequacy factor (load multiplier) for each load position and the respective failure mode. The minimum adequacy factor found for Leça bridge lead to a formation of a 4-hinge mechanism when the load is applied near ¼ arch span. A minimum adequacy factor of 2.5 was obtained for this model with unitary width. An equivalent factor of 8 is found when considering 3.1 meters for the transversal width of the bridge.
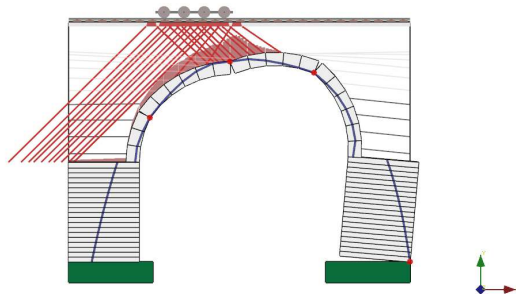

Figure 6. 4-hinge mechanism obtained for Leça bridge model with RING software

4.1 Results of service loading (DL+1P)

The response parameters of the 3D FE model is shown in Figure 7 in terms of the results of the maximum principal stresses (mainly tensile) and minimum principal stresses (mainly compressive) for the load level of the bridge weight and the vehicle with the intensity of 1P, where P represents the nominal vehicle load. The results reflect the level of stress under service loads (reference loading). The maximum tensile stress occurs in the spandrel wall with a value of 0.19 MPa and the maximum compressive stress occurs at the arch with 1 MPa. A value of about 500 kPa was found for

tension at the base considering only the self-weight of the bridge. For this load level, it was verified that the bridge response is still in the elastic domain and no plastic deformation was achieved in this step of the analysis.
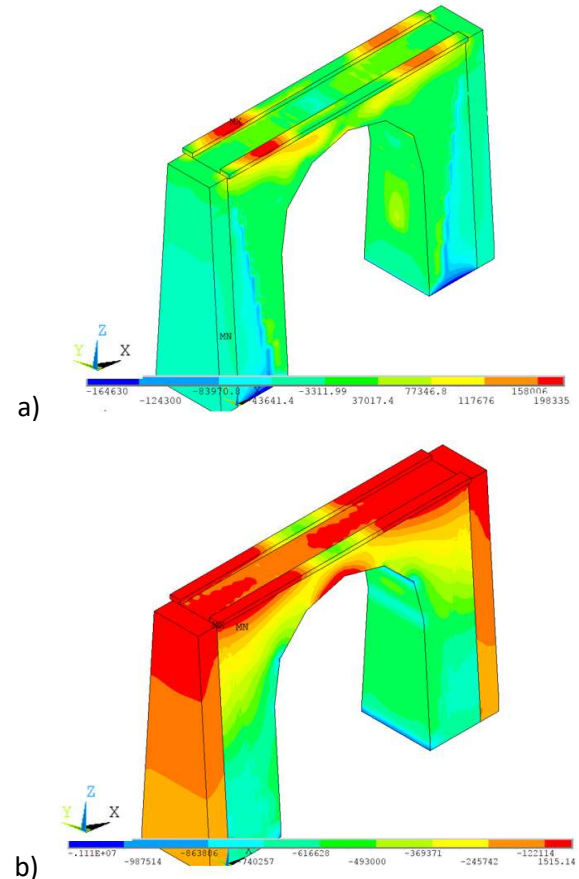

a)

b)

Figure 7. 3D model of Leça bridge - Stress level in the bridge deformed configuration under service conditions (DL+1P): (a) maximum principal stresses (in Pa) and (b) minimum principal stresses (in Pa).

4.2 Results of plastic evolution and maximum loading (DL+10P)

The structural response of the bridge 3D FE model for the load level of the bridge weight and the vehicle with the intensity of 10P (the maximum force applied) is shown in Figure 8. The results show the deformed configuration and the level of stress, in terms of maximum principal stresses and minimum principal stresses, for this step of loading, zooming the bridge area consisted only by the arch, spandrel wall and infill.

Table 3 summarizes the corresponding response values of the bridge model when the maximum

intensity level was applied, 10P. Aiming for comparison, the results of intensity levels 1P and 5P are also included in Table 3.
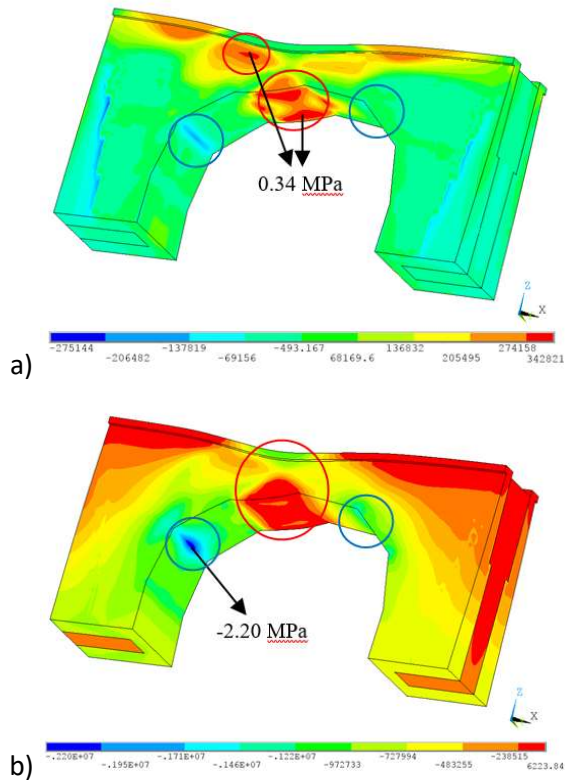

Figure 8. 3D sub-model of Leça bridge - stress level in the arch, spandrel and infill for the final loading step (DL+10P): (a) maximum principal stresses (in Pa) and (b) minimum principal stresses (in Pa)

Table 3. Response parameters in the arch, spandrel walls and infill: displacements and principal stresses

Level of intensity	Element	dv [mm]	σ_1^+ [MPa]	σ_3^- [MPa]
DL+1P	Arch	8.11 (dz)	0.18	-1.08
	Spandrel	0.20 (dy)	0.22	-0.66
	Infill	8.20 (dz)	0.05	-0.14
DL+5P	Arch	11.61 (dz)	0.31	-1.54
	Spandrel	0.51 (dy)	0.33	-0.97
	Infill	12.30 (dz)	0.15	-0.45
DL+10P	Arch	18.30 (dz)	0.34	-2.20
	Spandrel	1.02 (dy)	0.34	-1.50
	Infill	19.62 (dz)	0.24	-0.86

The maximum displacement in the crown of the arch is around 20 mm. Both maximum and minimum principal stresses occur in the arch with values of 0.34 MPa and -2.20 MPa, respectively. For this intensity load level, the response of masonry of the arch and the spandrel walls exhibit nonlinearity, as detailed in following paragraphs by the analysis of the plastic strain evolution.

Figure 9 and 10 show the state of plasticity in terms of its principal components in the bridge sub-model that includes the arch, spandrel walls and infill. The figures allow observing the plasticity evolution for the intensity levels of 5P and 10P. Table 4 summarizes the corresponding values for the plastic strains in the maximum and minimum principal directions obtained for the three different intensity levels considered in the bridge analysis.
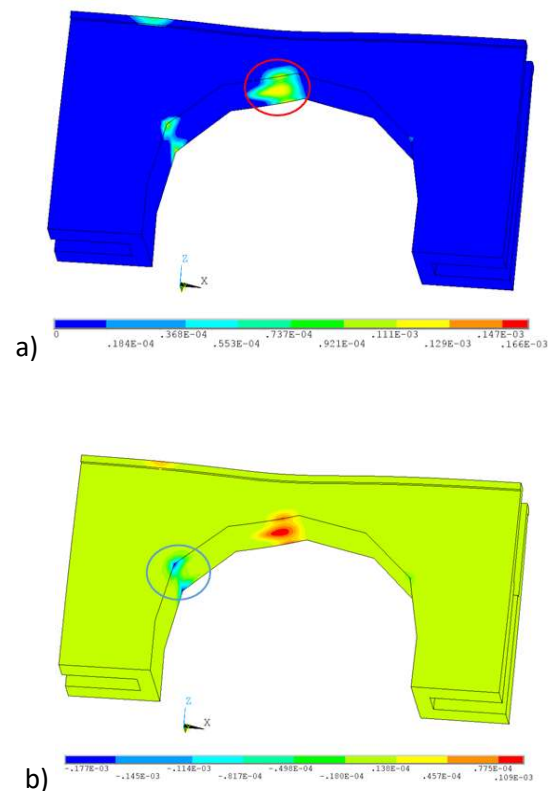

Figure 9. 3D sub-model of Leça bridge – plastic strain level for the load step (DL+5P): a) principal maximum strain and b) minimum plastic strain
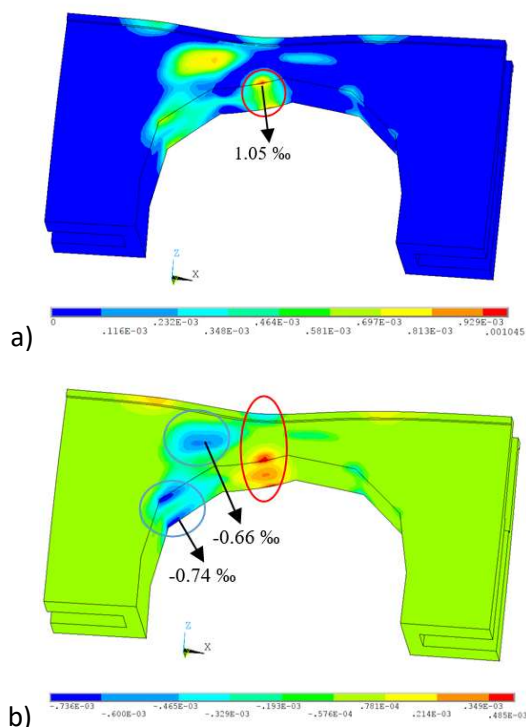
Figure 10. 3D sub-model of Leça bridge – plastic strain level for the final loading step (DL+10P): a) principal maximum strain and b) minimum plastic strain

Table 4. Principal plastic strains for the arch, spandrel wall and infill

Level of intensity	Element	*dv* [mm]	ε_{p1}^{+} [‰]	ε_{p3}^{-} [‰]
DL+1P	Arch	8.11 (dz)	0.00	0.00
	Spandrel	0.20 (dy)	0.00	0.00
	Infill	8.20 (dz)	0.00	0.00
DL+5P	Arch	11.61 (dz)	0.13	-0.18
	Spandrel	0.51 (dy)	0.16	-0.12
	Infill	12.30 (dz)	0.00	0.00
DL+10P	Arch	18.30 (dz)	1.05	-0.74
	Spandrel	1.02 (dy)	0.83	-0.66
	Infill	19.62 (dz)	0.00	0.00

By analysing the Figure 9, corresponding to a load level of 5P, is possible to identify one plastic hinge forming near the crown of the arch (marked with a red circle), which is consistent with the tensile stresses found for this load level, 0.31 MPa. In

another zone in the arch intrados (marked with a blue circle) considerable plastic deformations are found, resulted from the concentration of compressive stresses found at this level. For the maximum applied force 10P, shown in Figure 10, the plastic deformations are increasing in the mentioned zones in the arch, and for a new zone in the spandrel walls considerable plastic deformations are developing (marked with a blue circle), which is consistent with the high stresses found in this area for this intensity load level. No plastic deformation was found in the backfill zones.

4.3 Discussion

The analysis of the bridge response allowed recognizing two vulnerable zones influenced by both basic failure modes of stone arch bridges: the hinges mechanism in the arch and the crushing and out-of-plane of the spandrels.

A first estimation of the load-carrying capacity was obtained with RING software and a load multiplier of 8 was found for a 4-hinge failure mechanism in the arch when the load is applied load between near the ¼ span of the arch.

The results obtained with the 3D FE bridge model for the maximum applied force, 10 P, does not represent a conventional hinges mechanism formation in the arch. Instead, the failure occurred through a combination of one plastic hinge located in the arch near the crown under the loading zone, and by the crushing and out-of-plane movement in both spandrel walls in the area below the loading zone. The values for the displacements reached in the crown of the arch are relatively high, approximately 20 mm (1/800 of the span arch).

These results tend to show that the infill material usually found in railway masonry bridges, constituted by a cement mixture of irregular stones, forming a poorly masonry material, with a higher strength than the typical granular soil, have an important role in determining the failure mode of these bridges. The infill material is restraining the deformation of the arch, preventing the formation of a failure hinge mechanism in the arch, and therefore allowing higher forces to be applied before failure. The failure is conditioned by the

longitudinal and transversal behaviour of the spandrel walls in the area below the loading zone.

5. Conclusions

This paper focused on the numerical assessment of the load-carrying capacity of Leça railway bridge, based on a 3D FE global model and through incremental static loading.

The numerical responses of the bridge under dead-load and incremental vertical forces were evaluated and allowed to simulate the failure mode of the bridge and the corresponding vertical loading. The lower value found for the RING code model is an evidence of a more conservative approach resulting in the use of limit state methodology. The reasonably high values of the load multipliers obtained is an evidence of the good performance of this type of bridges under static loading.

Additionally, sensitivity analyses for the material parameters adopted for the infill and masonry can be done in order to study different numerical responses of the bridge. The dynamic effects due to the train loads will also be evaluated in the bridge's response.

6. Acknowledgements

7. References

[1] SB. Masonry arch bridges. Background document D4.7. Sustainable Bridges, 2007, EU FP6.

[2] Arêde, A., Costa, C., Gomes, A. T., Menezes, J. E., Silva, R., Morais, M. & Gonçalves, R. Experimental characterization of the mechanical behaviour of components and materials of stone masonry railway bridges. *Construction and Building Materials*. 2017; **153**, 663-681.

[3] AUTODESK. AutoCAD LT®2018.

[4] Ribó, R., Pasenau, M., Escolano, E., Ronda, J. & González, L. GiD reference manual. CIMNE, Barcelona, 2018.

[5] ANSYS. Academic Research, Release 18.1, Ansys Fluent Theory Guide, 2017.

[6] CEN. EN1991-2: Actions on structures-Part 2: Traffic loads on bridges. 6, 2003.

[7] Silva, R., Costa, C., Arêde, A. Experimental and numerical approaches for calibration of the material parameters used in models of stone masonry railway bridges. Fourth International Conference on Railways Technology, Railways 2018, 3-7 September, Stiges, Spain, 2018.

[8] LIMITSTATE RING. ring3.2b software, 2016.